THE JOURNAL OF BIOLOGICAL CHEMISTRY VOL. 284, NO. 28, pp. 19043–19052, July 10, 2009

Structural Basis for Ubiquitin Recognition by a Novel Domain from Human Phospholipase A_2-activating Protein*[S]

Received for publication, April 16, 2009 Published, JBC Papers in Press, May 7, 2009, DOI 10.1074/jbc.M109.009126

Qing-Shan Fu[‡§], Chen-Jie Zhou[‡], Hong-Chang Gao[¶], Ya-Jun Jiang[‡§], Zi-Ren Zhou[‡§], Jing Hong[¶], Wen-Ming Yao[¶], Ai-Xin Song[‡], Dong-Hai Lin[¶1], and Hong-Yu Hu[‡2]

From the [‡]State Key Laboratory of Molecular Biology, Institute of Biochemistry and Cell Biology, Shanghai Institutes for Biological Sciences, Chinese Academy of Sciences, Shanghai 200031, the [¶]Shanghai Institute of Materia Medica, Shanghai Institutes for Biological Sciences, Chinese Academy of Sciences, Shanghai 201203, and the [§]Graduate School of the Chinese Academy of Sciences, Beijing 100039, China

Ubiquitin (Ub) is an essential modifier conserved in all eukaryotes from yeast to human. Phospholipase A_2-activating protein (PLAA), a mammalian homolog of yeast DOA1/UFD3, has been proposed to be able to bind with Ub, which plays important roles in endoplasmic reticulum-associated degradation, vesicle formation, and DNA damage response. We have identified a core domain from the PLAA family ubiquitin-binding region of human PLAA (residues 386–465, namely PFUC) that can bind Ub and elucidated its solution structure and Ub-binding mode by NMR approaches. The PFUC domain possesses equal population of two conformers in solution by *cis*/*trans*-isomerization, whereas the two isomers exhibit almost equivalent Ub binding abilities. This domain structure takes a novel fold consisting of four β-strands and two α-helices, and the Ub-binding site on PFUC locates in the surface of α2-helix, which is to some extent analogous to those of UBA, CUE, and UIM domains. This study provides structural basis and biochemical information for Ub recognition of the novel PFU domain from a PLAA family protein that may connect ubiquitination and degradation in endoplasmic reticulum-associated degradation.

The eukaryotic secreted proteins are translocated into the endoplasmic reticulum after synthesis in cytosol. Misfolded or abnormally assembled proteins should be targeted for degradation through the endoplasmic reticulum-associated degradation (ERAD)[3] pathway (1, 2). This pathway involves many molecular steps: unfolded protein response in the endoplasmic reticulum lumen, retrotranslocation back into the cytosol, ubiquitin (Ub) conjugation, delivery of ubiquitinated proteins to proteasome, and degradation of the substrates by proteases (3, 4).

A yeast protein DOA1/UFD3 has been shown to bind to CDC48 by both indirect and direct ways (5–7), suggesting that DOA1 may be involved in ERAD. Evidence indicates that DOA1 directly competes with UFD2 at the same docking site on CDC48, which determines whether a substrate is multiubiquitinated and routed to the proteasome for degradation or deubiquitinated and released for other purposes (8). The direct interaction between DOA1 and Ub was suggested by recent studies (7, 9). Moreover, DOA1 also plays roles in the monoubiquitination of histone H2B and proliferating cell nuclear antigen (10) and in sorting ubiquitinated membrane proteins into multivesicular bodies (11).

The mammalian homolog of DOA1 is called phospholipase A_2-activating protein (PLAA), which can bind to P97/VCP (a CDC48 homolog) with its C-terminal domain PUL (7). Having high sequence similarity (31% identity) with DOA1, PLAA is proposed to possess similar function of DOA1. Like DOA1, PLAA has an N-terminal WD40 domain with yet unknown function. The central region of PLAA contains a putative PLAA family ubiquitin-binding (PFU) domain, which is supposed to bind with Ub as observed in yeast DOA1 (7). Although the mechanism underlying the function of PLAA remains unclear, Ub binding of PLAA might be the central role that connects ubiquitination and degradation in ERAD. Thus, elucidating the molecular mechanism for specific binding of PLAA with Ub is prerequisite for understanding the function of PLAA as well as DOA1. To further understand the Ub-binding mechanism by which PLAA functions in ERAD pathway, we identified a small Ub-binding domain from human PLAA (12) and elucidated the domain structure and Ub-binding properties by NMR and mutagenesis approaches.

EXPERIMENTAL PROCEDURES

Protein Expression and Purification—The DNA sequences encoding UIM-PFU (residues 312–465), PFU (residues 340–465), and PFUC (residues 386–465) were cloned into the pET-32 M vector through BamHI/XhoI sites. For convenience of NMR assignments, PFU or PFUC was renumbered from 3 or 49 to 128 according to amino acid residues of the PFU domain. All of the mutants of PFUC were generated via PCR and cloned into the pET-32 M vector, which produces Trx-fused proteins.

* This work was supported by National Basic Research Program of China Grants 2006CB910305, 2006CB806508, and 2007CB914304 and National Natural Science Foundation of China Grants 30600103 and 30670431.

The atomic coordinates and structure factors (codes 2K89, 2K8A, 2K8B, and 2K8C) have been deposited in the Protein Data Bank, Research Collaboratory for Structural Bioinformatics, Rutgers University, New Brunswick, NJ (http://www.rcsb.org/).

[S] The on-line version of this article (available at http://www.jbc.org) contains supplemental Figs. S1–S4 and Table S1.

[1] To whom correspondence may be addressed. E-mail: dhlin@mail.shcnc.ac.cn.

[2] To whom correspondence may be addressed. E-mail: hyhu@sibs.ac.cn.

[3] The abbreviations used are: ERAD, endoplasmic reticulum-associated degradation; PLAA, phospholipase A_2-activating protein; Ub, ubiquitin; PFU, PLAA family ubiquitin-binding; PFUC, PFU core domain; NEDD8, neural precursor cell expressed, developmentally down-regulated 8; GST, glutathione *S*-transferase; HSQC, heteronuclear single quantum coherence.

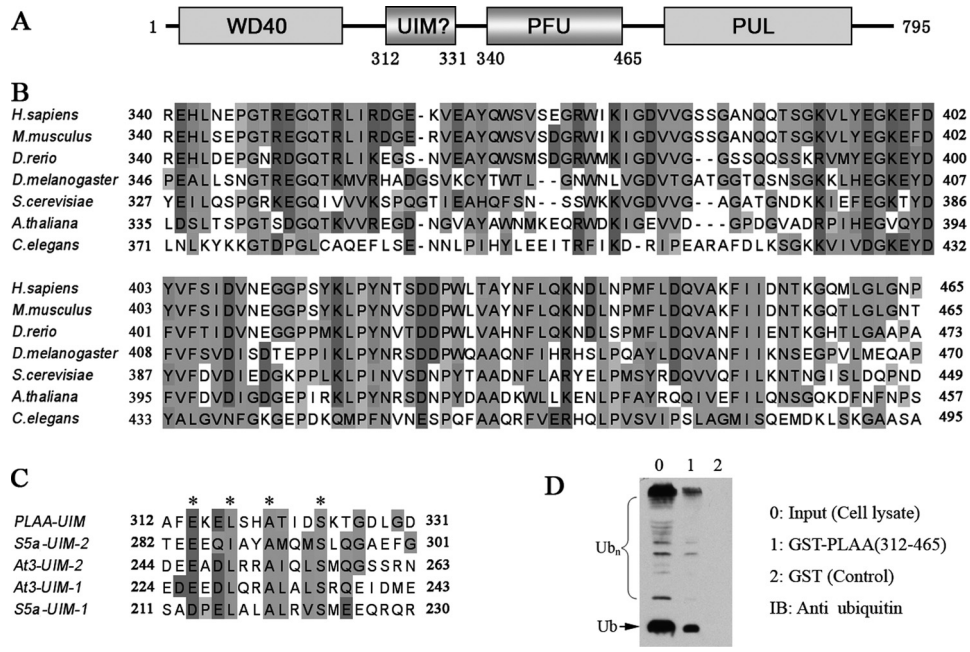

FIGURE 1. **PLAA harbors a central region that putatively interacts with Ub.** *A*, domain architecture of PLAA. *WD40*, WD40 repeats; *PUL*, PLAA, UFD3, and LUB1 conserved domain; *UIM*, ubiquitin-interacting motif. *B*, multiple sequence alignment of the PFU domain from different species. *C*, the putative UIM sequence has the conserved residues Glu, Leu, Ala, and Ser as marked by *asterisks*. *S5a*, S5a subunit of proteasome; *At3*, ataxin-3. *D*, GST pulldown assay for the central region of PLAA (residues 312–465, UIM-PFU) binding with Ub. The products pulled down from 293T cell lysate were detected by Western blotting with an anti-Ub antibody.

These proteins were overexpressed in *Escherichia coli* strain BL21(DE3) and purified by Ni^{2+}-nitrilotriacetic acid affinity columns (Qiagen), followed by on-column cleavage of the Trx tag by thrombin. UIM (312–331) was cloned into the pGBTNH vector through BamHI/XhoI sites, which produces a GB1-fused protein (13). GB1-UIM was purified through a Ni^{2+}-nitrilotriacetic acid affinity column. UIM-PFU was also cloned into the pGEX-4T-3 vector to produce a GST-fused protein. GST-UIM-PFU was purified through a glutathione affinity column. All of the proteins were further purified by Superdex 75 gel filtration chromatography (GE Healthcare). The procedure for expression and purification of NEDD8 was similar to that for Ub. SUMO-1 was prepared from a GST-fused form followed by thrombin cleavage.

Chemical Shift Perturbation Experiments—Two-dimensional ^1H-^{15}N HSQC spectra of ^{15}N-labeled Ub (~200 μM) in an NMR buffer (20 mM phosphate, 50 mM NaCl, 0.01% NaN_3, pH 6.5) were recorded at different points of titration with the PLAA fragments, including UIM-PFU, GB1-UIM, PFU, and PFUC and its mutants. ^{15}N-Labeled PFUC and P77A mutant were dissolved into the same buffer to a concentration of about 200 μM, and different amounts of unlabeled Ub or Ub-like proteins were added with each step monitored by acquiring a two-dimensional ^1H-^{15}N HSQC spectrum. The average chemical shift changes ($\Delta\delta$) were used for the binding assay and for the calculation of dissociation constants (K_D) (14).

NMR Spectroscopy and Structure Determination—The PFU and PFUC samples (~1 mM) were dissolved into the NMR buffer (20 mM phosphate, 50 mM NaCl, and 0.01% NaN_3, pH 6.5), and the spectra were recorded at 25 °C on a 600-MHz Varian Unity Inova spectrometer. Backbone and side chain assignments were completed by analyzing the following spectra: HNCACB, CBCA(CO)NH, HNCO, HNHA, C(CO)NH, H(CCO)NH, and HCCH-TOCSY. Total dihedral angle restraints (Φ/Ψ) were obtained from chemical shifts of $^1H_\alpha$, $^{13}C_\alpha$, $^{13}C_\beta$, and ^{13}CO using TALOS (15). Three-dimensional ^{15}N- and ^{13}C-edited nuclear Overhauser effect spectroscopy spectra were acquired to provide the distance restraints for structure computation by using ARIA2.0 (16). A family of 200 structures was calculated using the simulated annealing protocol, and 15 of the lowest energy structures were selected. Structure assessment was performed by PROCHECK (17).

The structure of PFUC-Ub complex was calculated based on chemical shift perturbation data by using HADDOCK software (18). Fifteen NMR structures of PFUC and one crystal structure of Ub (Protein Data Bank code 1UBQ) were used for mapping the interfaces and docking the structures. The solvent accessibilities of different amino acid residues were calculated by the NACCESS program. Residues with average chemical shift changes ($\Delta\delta$) greater than the mean value and with high solvent accessibilities were selected as the active residues, whereas the solvent-accessible surface neighbors of these active residues were defined as passive residues. An ambiguous distance restraint of 3.0 Å was invoked between all active residues in one molecule to any atoms within the active and passive residues of the other partner. Initially, 1000 complex structures were generated by rigid body energy minimization, and the best 200 structures with the lowest energy were selected for torsion angle dynamics and Cartesian dynamics calculation in an explicit water solvent. It totally produced one major cluster of about 30 structures.

GST Pulldown Assay—Glutathione-Sepharose beads (30 μl) were washed three times with 500 μl of phosphate-buffered saline (20 mM phosphate, 100 mM NaCl, 10 mM KCl, pH 7.3), then incubated with 500 μl of GST-UIM-PFU (200 μM, in the phosphate-buffered saline buffer) for 30 min at 4 °C, and washed two times with the same buffer to remove the unbound protein. Whole cell lysate from HEK 293T cells was centrifuged at 12,000 × *g* for 15 min. 1 ml of the supernatant was incubated with GST-UIM-PFU-conjugated beads for 30 min. After being washed with 200 μl of the phosphate-buffered saline buffer, the beads were then further washed with 50 μl of the washing buffer (10 mM reduced glutathione, 50 mM Tris-HCl, pH 8.0). Eventually, 40 μl of the sample eluted from the beads was subjected to Western blotting analysis. GST protein was set as a control.

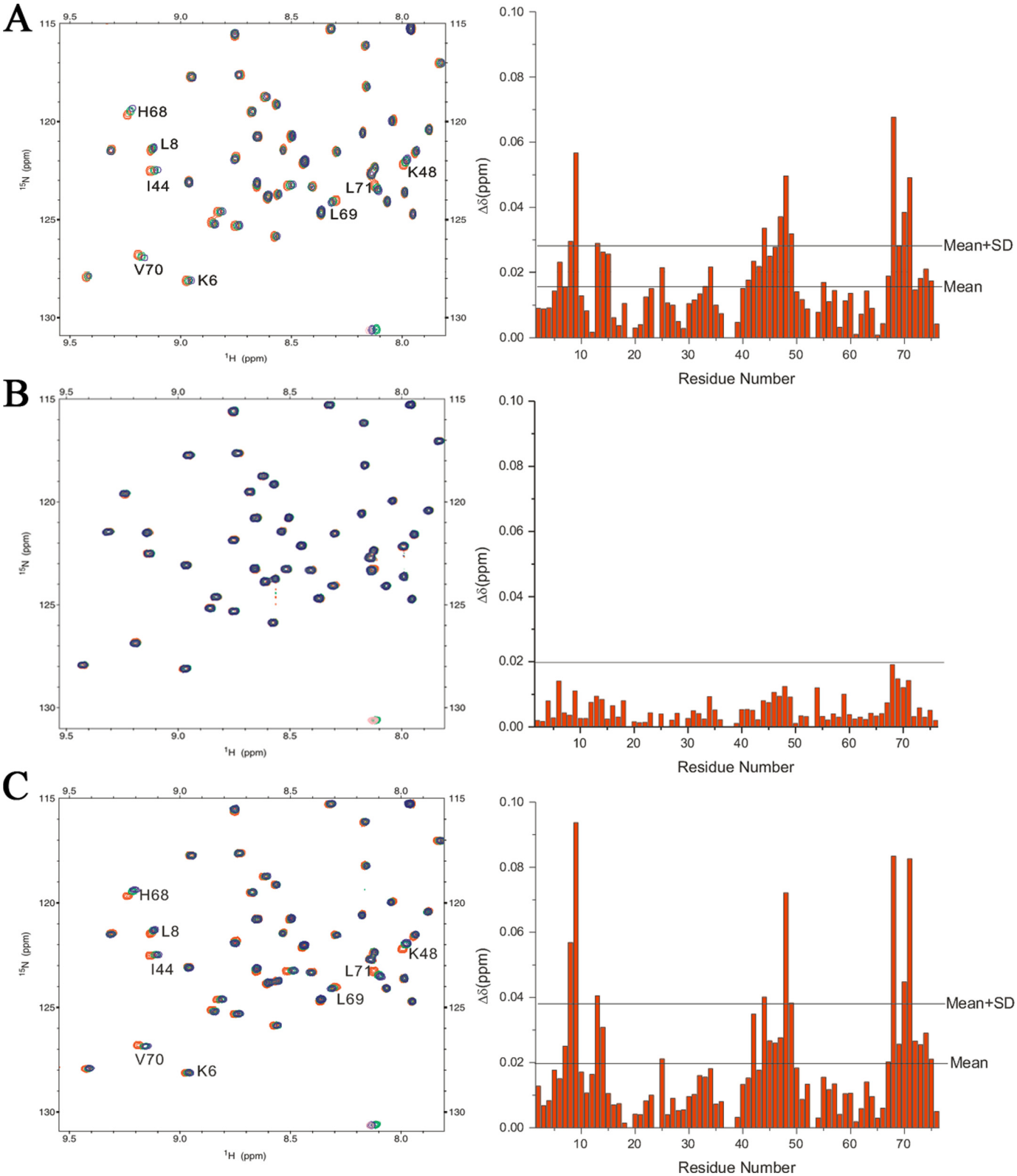

FIGURE 2. **Chemical shift perturbation analysis reveals the Ub-binding region of PLAA.** *A*, *left panel*, overlay of the ^{1}H-^{15}N HSQC spectra of ^{15}N-labeled Ub in free form and upon titration with UIM-PFU. The Ub/UIM-PFU molar ratios are 1:0 (*red*), 1:2 (*green*), and 1:4 (*blue*), respectively. *Right panel*, diagram of the chemical shift changes (Δδ) of Ub against residue number at a molar ratio of 1:4. *B* and *C*, as in *A*, ^{15}N-labeled Ub upon titration with GB1-UIM (*B*) or PFU (*C*). The GB1 tag was applied to easily express and purify the UIM peptide.

RESULTS

The Domain Architecture and Sequence Alignment of PLAA—PLAA is a homologous protein of yeast DOA1 (7). These proteins share a similar domain architecture (Fig. 1*A*), consisting of an N-terminal WD40 domain of seven repeats, a central region, and a C-terminal PUL domain that can bind to CDC48 or P97

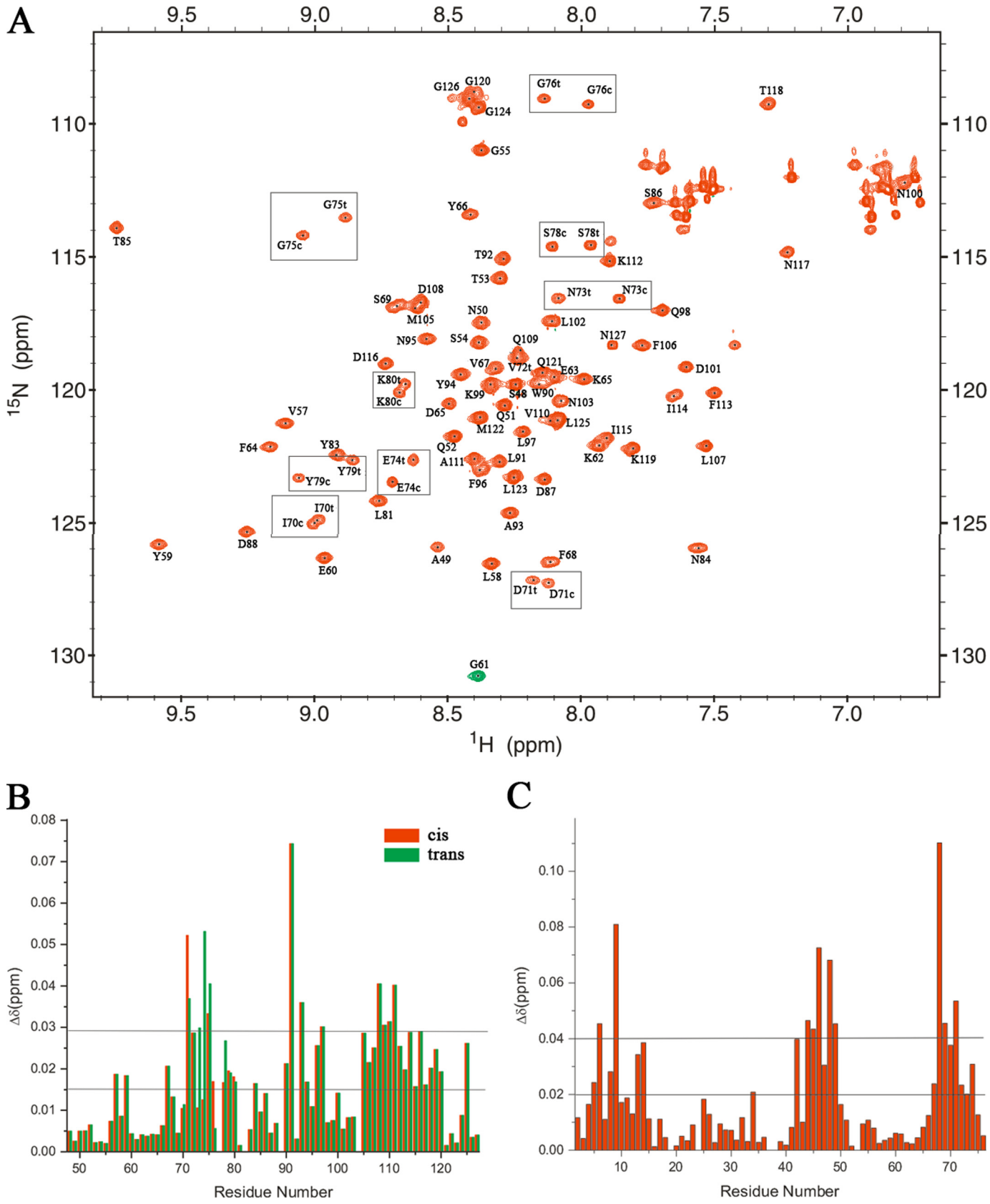

FIGURE 3. **Backbone chemical shift assignment of the PFUC domain showing *cis*/*trans* isomerization and Ub binding.** *A*, ^{1}H-^{15}N HSQC spectrum of PFUC with assigned resonance peaks. The peaks in *rectangles* indicate the duplicate signals that originate from *cis*/*trans*-isomerization of proline residues. *B*, diagram of the chemical shift changes (Δδ) of PFUC against its residue number at a PFUC/Ub molar ratio of 1:4. The changes in the *cis*-isomer are shown in *red bars*, and those in the *trans* form are in *green*. The *two horizontal lines* indicate mean Δδ and mean Δδ plus S.D. values. *C*, diagram of the chemical shift changes (Δδ) of Ub against its residue number. ^{15}N-Labeled Ub was titrated with PFUC at a Ub/PFUC molar ratio of 1:4.

(5). The central region contains a PFU domain with high sequence homology (Fig. 1*B*), which was previously proposed to bind with Ub (7). Interestingly, sequence alignment shows a conserved region in between WD40 and PFU of human PLAA (residues 312–331) that is homologous to the UIM motifs (Fig. 1*C*). The UIM motifs from S5a subunit of proteasome (19, 20) and ataxin-3 (21) are capable of binding with Ub and ubiquitinated substrates, in which the conserved residues Leu, Ser, and especially Ala (22) are critical for the binding (23–25). This implies that, in addition to the PFU domain, the putative UIM motif of PLAA may provide an alternative candidate for binding with Ub.

The PFU Domain of PLAA Binds with Ub—It was previously reported that yeast DOA1 binds with Ub through its central PFU domain (7). By GST pulldown assay, we confirmed that this corresponding region of PLAA (residues 312–465, UIM-PFU) including the putative UIM motif and the PFU domain can bind with mono-Ub, poly-Ub and/or ubiquitinated proteins from cell lysate (Fig. 1*D*). This suggests that either PFU or probably UIM of PLAA serves as the Ub-binding domain as observed in that of yeast DOA1.

To clarify which domain or motif in this region binds with Ub, we labeled Ub with ^{15}N and performed chemical shift perturbation experiments by titration of the three fragments of PLAA: UIM-PFU (residues 312–465), GB1-UIM (residues 312–331), and PFU (residues 340–465), respectively. As expected, the UIM-PFU titration causes significant chemical shift changes of the residues in Ub (Fig. 2*A*), further corroborating that the central region of PLAA can bind with Ub. However, the putative UIM motif cannot bind with Ub, for no significant change occurs in the ^{1}H-^{15}N HSQC spectra of Ub upon its titration (Fig. 2*B*). By contrast, titration of Ub with PFU also results in chemical shift changes of residues Leu^{8}, Ile^{44}, His^{68}, and Val^{70} (Fig. 2*C*) that construct a canonical binding surface on Ub (12), strongly supporting that the PFU domain in PLAA possesses Ub binding ability.

A Novel Ub-binding Domain from PLAA—Because the PFU domain can bind with Ub, we labeled this fragment (PLAA(340–465) or PFU(3–128)) with $^{15}N/^{13}C$ and partially assigned the backbone resonances. The ^{1}H-^{15}N HSQC spectrum of the PFU fragment is well dispersed, indicating a well folded domain in this fragment (supplemental Fig. S1). However, the backbone resonances of the N-terminal residues exhibit relatively low intensities or peak missing. The three-dimensional ^{15}N- or ^{13}C-edited nuclear Overhauser effect spectroscopy spectra also exhibit few nuclear Overhauser effect spectroscopy signals among the N-terminal residues (data not shown). These all suggest that the N-terminal region of the PFU fragment is flexible and does not adopt a defined conformation. Moreover, titration of the PFU fragment with Ub results in chemical shift perturbation mostly on the C-terminal residues, suggesting that the Ub-binding sites on PFU are located in its C terminus (supplemental Fig. S1). We thus subcloned the Ub-binding domain from PLAA (namely PFUC for PFU core domain, PLAA(386–465)) and determined its solution structure by NMR. The ^{1}H-^{15}N HSQC spectrum of PFUC also exhibits well dispersed and homogenous (Fig. 3*A*). Most of the peaks of PFUC reside in the same positions as they do in the spectrum of PFU (supplemental Fig. S1), indicating that PFUC possesses a compact structure as in the PFU fragment. Again, chemical shift perturbation analysis demonstrates that PFUC still retains the ability to bind with Ub (Fig. 3, *B* and *C*), in which the Ile^{44} residue locates in the center of the canonical binding surface on Ub.

TABLE 1
Dissociation constants (K_D) for the binding affinities of PFU fragments and its mutants with Ub or Ub-like proteins

PUF and mutants	K_D[a]
	mM
UIM-PFU	0.99 ± 0.29
PFU	0.98 ± 0.28
PFUC wild type	1.8 ± 0.6[b]
cis/trans-P77A	1.4 ± 0.2[b]
WT	1.4 ± 0.3
Helix-1 L91A	1.0 ± 0.1
L97A	1.3 ± 0.4
Helix-2 M105A	2.8 ± 0.6
D108N	3.5 ± 0.9
M105A/D108N	>10
P77 loop D71N	1.5 ± 0.2
V72I	1.3 ± 0.4
V72F	1.1 ± 0.3
V72K	0.68 ± 0.16
V72D	0.64 ± 0.03
V72A	0.34 ± 0.08
V72G	0.54 ± 0.07
Ub-like with PFUC	
NEDD8	2.2 ± 0.7[c]
SUMO-1	>10[c]

[a] The data were obtained from titration of ^{15}N-labeled Ub with different PFU fragments and mutants. The data are presented as the means ± M.D. (M.D., mean deviation of data from 3 or more amino acids which come from a single NMR titration experiment).
[b] The data were from titration of ^{15}N-labeled PFUC with Ub.
[c] The data were from titration of ^{15}N-labeled PFUC with Ub-like proteins.

To compare the binding abilities of these PLAA fragments, we performed titration of ^{15}N-labeled Ub with UIM-PFU, PFU, and PFUC, respectively, and determined their dissociation constants (K_D) (see Fig. 6*A*). The binding of these three fragments with Ub is relatively weak with same affinities of millimolar range (Table 1). This result demonstrates that the core domain of PFU retains the Ub binding activity and implies that the PFUC domain represents most of the properties of the PFU fragment structurally and functionally.

NMR Structures of PFUC in Solution: the Proline cis/trans-Isomerization—We assigned all the chemical shifts of the PFUC domain by NMR. Interestingly, residues 70–80 exhibit duplicate peaks in the ^{1}H-^{15}N HSQC spectrum (Fig. 3*A*), as they do in that of PFU (supplemental Fig. S1), indicating that there are two conformers in solution with slow exchange. The Gly^{76}–Pro^{77} prolyl bond exists both in the *cis*- and *trans*-conformations as evidenced by the characteristic nuclear Overhauser effect correlations between Gly^{76} and Pro^{77}, as well as the $^{13}C_{\beta}$ and $^{13}C_{\gamma}$ chemical shifts of Pro^{77} (supplemental Fig. S2) (26). Judging from the signal intensities, the two sets of resonance peaks show a population ratio of about 1:1 (50.3% *cis versus* 49.7% *trans*), suggesting that the *cis*- and *trans*-conformers have the same free energy level. To our knowledge, this is the first illustration of a protein with equal population of the *cis*- and *trans*-isomers in solution. Normally, the *cis*-isoform of a protein occurs with a very low population (5% or so) or is scarcely observed in solution. On the other hand, mutation of Pro^{77} (P77A) results in only one set of peaks for residues 70–80

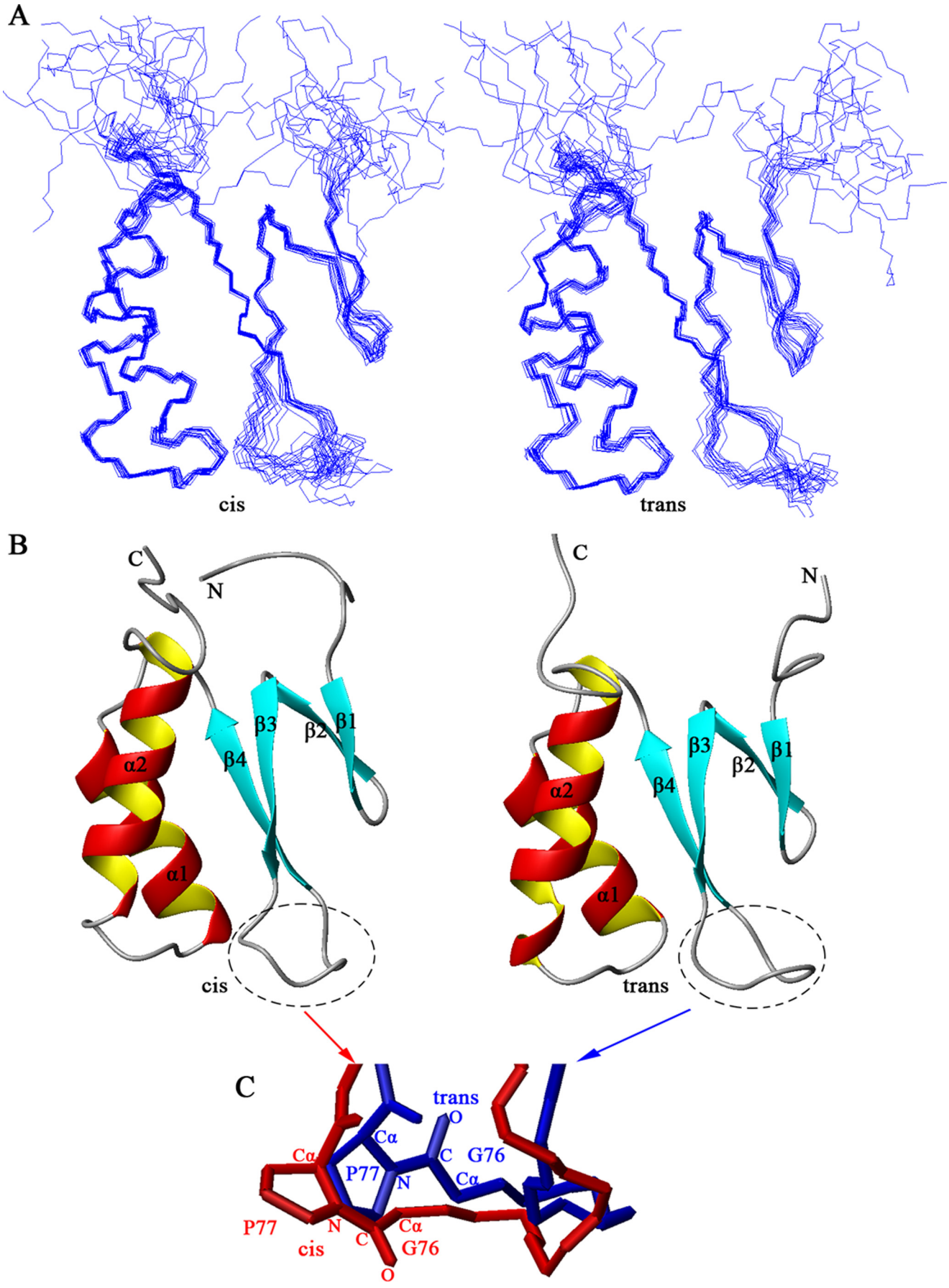
A
cis
trans
B
C
N
α2
α1
β4
β3
β2
β1
cis
trans
C
trans
O
Cα
C
G76
P77
N
Cα
Cα
P77
N
C
Cα
cis
G76
O

in the ^{1}H-^{15}N HSQC spectrum (supplemental Fig. S2). This confirms that the Gly^{76}–Pro^{77} prolyl bond is the main source for the conformational heterogeneity of the PFUC domain in solution.

We then performed titration of ^{15}N-labeled PFUC and its P77A mutant with different amounts of Ub (Fig. 6*B*). The dissociation constants (K_D) are 1.8 ± 0.6 and 1.4 ± 0.2 mM for WT PFUC and P77A, respectively (Table 1). Although an ensemble of equal population of *cis*- and *trans*-PFUC binds with Ub relatively weakly, the all-*trans*-conformer of P77A mutant binds Ub with a similar affinity, suggesting that both *cis*- and *trans*-conformers have equivalent Ub binding ability.

Solution Structures of PFUC Reveal a Novel Domain Fold—We then obtained two sets of distance restraints for each isomer of PFUC from ^{15}N- and ^{13}C-edited nuclear Overhauser effect spectroscopy spectra, and calculated the structures of *cis* and *trans* conformers independently. A summary of the NMR experimental restraints for structural calculation and statistics for both conformers is presented in supplemental Table S1. Fig. 4*A* shows an ensemble of the 15 lowest energy structures superimposed on the backbones for the two conformers. Both *cis*- and *trans*-isomers fold into a compact globular domain of ($\alpha + \beta$) pattern consisting of four β-strands and two α-helices (Fig. 4*B*). The four β-strands, β1, β2, β3, and β4, arrange into two separate anti-parallel β-sheets. The meander between β2 and β3 contains only one residue of Asp^{65}, and the angle between them is about 60°. However, there are hydrophobic contacts between Val^{57} in β1 and Val^{67} in β3 (supplemental Fig. S3), probably stabilizing the atypical fold. The two α-helices arrange at an angle about 45° to each other and keep in contact with the β-sheet of β3 and β4 (Fig. 4*B*). The major difference of the backbone structures between the *cis*- and *trans*-conformers lies in the loop of Ile^{70}–Lys^{80} around Pro^{77} (P77 loop) connecting the β3 and β4 strands (Fig. 4*C*).

Sequence analysis indicates that there is no homologous sequence of the known structure in Protein Data Bank data base with that of PFUC. By using the DALI server (27), we identified a most similar structure (Protein Data Bank code 1G2R, Z = 3.5) of a hypothetical protein YlxR (28). This structure shows a folding pattern partially similar with that of PFUC, but the $\beta1\beta2$ sheet in PFUC is missing in the 1G2R structure (supplemental Fig. S3). Although the $\beta1\beta2$ sheet displays a little apart from the core pattern (β-flap), it still contacts with the $\beta3\beta4$ sheet by hydrophobic interactions (supplemental Fig. S3). This structure is not consistent with the previous prediction that PFU may have structural homology with the UEV domain (7, 12). Because there is no similar structure deposited in Protein Data Bank, the structure of PFUC could be considered as a novel domain fold.

Structural Model of the PFUC-Ub Complex—The clear delineation of the binding interface between PFUC and Ub has been brought out by an NMR restraint-guided docking approach (HADDOCK) (18). Fig. 5*A* shows an overlay of 10 lowest interaction energy and water-refined structures. The root mean square deviation of all backbone atoms in the interfaces is 1.2 ± 0.8 Å for the *cis*-PFUC-Ub complex and 1.1 ± 0.9 Å for *trans*-PFUC-Ub. Both isomers of PFUC bind Ub on the canonical hydrophobic interfaces mainly constructed by α2-helix of PFUC and β-sheet of Ub. Met^{105} of PFUC is in close contact with the side chain of Ile^{44} of Ub by hydrophobic interactions, whereas Asp^{108} contacts with Arg^{42} possibly by electrostatic interactions (Fig. 5*B*). To confirm the binding mode of the PFUC-Ub complex, we performed mutagenesis of the residues that experience larger chemical shift changes upon Ub binding (Fig. 3*B*) and NMR titration experiments (Fig. 6). Mutation of the residues on α1-helix (L91A and L97A) does not significantly affect the binding, whereas mutation on α2-helix (M105A and D108N) shows increased K_D values to several millimolars (Fig. 6*C* and Table 1). In addition, double mutation of these residues

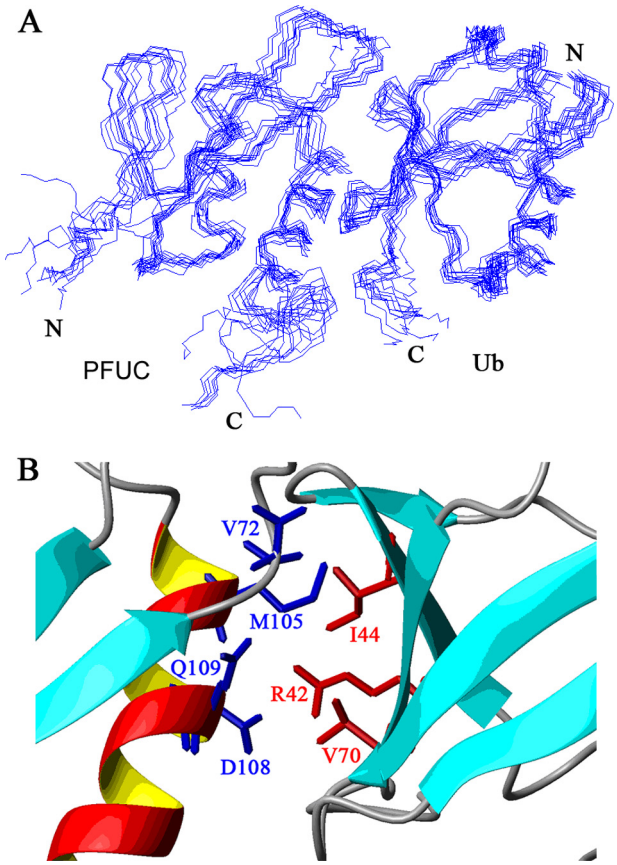

FIGURE 5. **HADDOCK-derived model for the PFUC-Ub complex.** *A*, backbone superposition of 10 refined *cis*-PFUC-Ub complex structures. The average energy for the cluster is −6349 ± 59 kcal·mol^{-1} for the *cis*-PFUC-Ub complex and that is −6377 ± 81 kcal·mol^{-1} for *trans*-PFUC-Ub. The root mean square deviation of all backbone atoms in the interfaces is 1.2 ± 0.8 Å for *cis*-PFUC-Ub and 1.1 ± 0.9 Å for *trans*-PFUC-Ub. *B*, close-up view of the interfaces showing the side chains of key interacting residues. The stick representations are in *red* for the side chains from Ub and in *blue* for those from PFUC.

FIGURE 4. **Solution structure of the PFUC domain.** *A*, backbone superposition of 15 lowest-energy structures in *cis* (*left panel*) and *trans* (*right panel*) isomers. *B*, ribbon representation of the structures for *cis* (*left panel*) and *trans* (*right panel*) isomers. N and C indicate the N and C termini of PFUC, respectively. *C*, comparison of the *cis* and *trans* isomers in the loop between β3 and β4 where Pro^{77} resides. The Gly^{76}–Pro^{77} prolyl bonds in both *cis*- and *trans*-isomers are fit together and the side chain positions of Gly^{76} and Pro^{77} are shown in *red* (*cis*) and *blue* (*trans*).

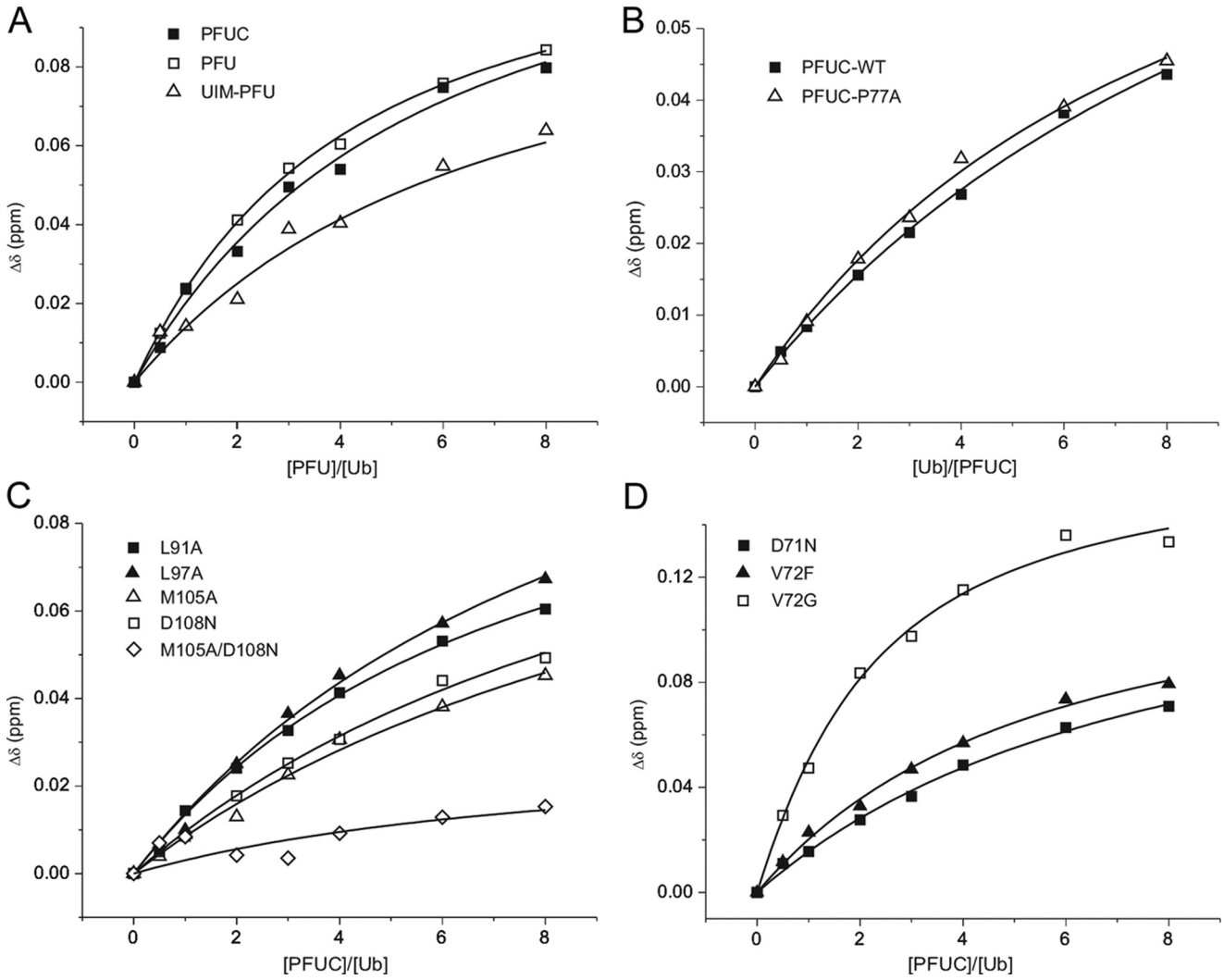

FIGURE 6. **Quantitative analysis of the Ub binding affinities of PFUC and its mutants.** *A*, titration of ^{15}N-labeled Ub with three PFU fragments, PFUC, PFU, and UIM-PFU. *B*, titration of ^{15}N-labeled wild-type and P77A mutant of PFUC with unlabeled Ub. *C*, titration of ^{15}N-labeled Ub with unlabeled PFUC mutants in α1-helix (L91A and L97A) and in α2-helix (M105A, D108N, and M105A/D108N). *D*, titration of ^{15}N-labeled Ub with unlabeled PFUC mutants in the P77 loop region (D71N, V72F, and V72G). The average chemical shift changes of Leu^{71} in Ub are shown in *A*, *C*, and *D*, and those of Ala^{111} in PFUC or the P77A mutant are shown in *B*.

almost abolishes the binding of PFUC with Ub, because the chemical shifts of residues on the canonical binding surface of Ub have no significant changes upon addition of the M105A/D108N mutant. This result demonstrates that PFUC binds Ub through the surface of its C-terminal α2-helix.

To define the binding specificity of the PFU core domain, we prepared two Ub-like proteins, NEDD8 and SUMO-1 and determined their binding affinities with PFUC (supplemental Fig. S4). As a result, NEDD8 exhibits similar binding affinity with Ub, whereas SUMO-1 has no PFUC binding ability (Table 1). NEDD8 shows high sequence and structural similarities with Ub, especially the conserved hydrophobic patch (Ile^{44}, Val^{70}, and Leu^{8}) (29). On the contrary, SUMO-1 is quite different from Ub in this characteristic surface; it is reasonable that SUMO-1 has lost the binding ability with PFUC. Therefore, the PFU core domain binds to the Ub-like proteins or domains weakly but specifically with a canonical mode via the conserved hydrophobic interfaces.

Effects of the P77 Loop Region on Ub Binding Ability—Some residues, such as Asp^{71} and Val^{72} in the P77 loop region, also show large chemical shift changes upon titration of Ub (Fig. 3*B*). To make clear whether these residues are involved in direct Ub binding, we performed mutations of Asp^{71} and Val^{72} and NMR titration experiments. As a result, D71N, V72I, and V72F mutants do not show change of their Ub binding affinities (Fig. 6*D* and Table 1), suggesting that the loop region is not directly involved in the Ub binding. Intriguingly, the mutants V72K, V72D, V72A, and V72G exhibit significantly enhanced Ub binding affinities (Fig. 6*D* and Table 1). The V72A and V72G mutations make the side chain smaller in the Val^{72} position, and the V72K and V72D mutations alter the charges in this position. These four mutations confer the loop more flexible, suggesting that the loop flexibility may considerably affect their Ub binding affinities. Thus, the results demonstrate that the P77 loop does not directly contact Ub but somehow affects PFUC binding with Ub.

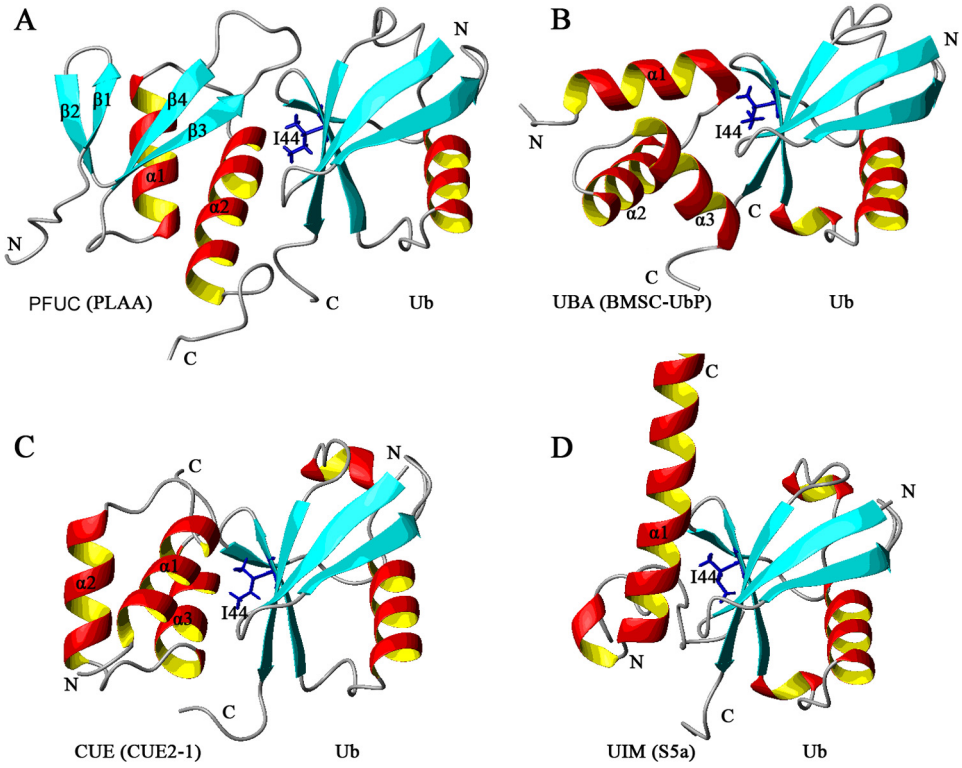

FIGURE 7. **Structural comparison of some Ub-binding domains complexed with Ub.** All of these Ub-binding domains bind with Ub through the surface mainly on α-helix. Ile[44] residue of Ub is shown in *blue stick*. The Ub receptors shown here are: *cis*-PFUC from PLAA (Protein Data Bank code 2K8B) (*A*); UBA from BMSC-UbP (Protein Data Bank code 2DEN) (*B*); CUE from Cue2–1 (Protein Data Bank code 1OTR) (*C*); and UIM from S5a subunit of proteasome (Protein Data Bank code 1YX5) (*D*).

DISCUSSION

It was previously reported that the PFU domain of yeast DOA1 binds with both mono- and poly-Ub (7). We have characterized the Ub binding specificity of PLAA by identifying a novel small domain that is distinct from other known Ub-binding domains in amino acid sequence and three-dimensional structure. Our structural and biochemical data suggest that this PFUC domain binds Ub through the surfaces mainly in the α-helical region with the Ub surface centered on the Ile[44] patch (12) (Fig. 5*B*).

Because Met[105], Asp[108], and Gln[109] all reside in the α2-helical region, we conclude that PFUC binds with Ub through the surface on the second α-helix (Fig. 7*A*), which is to some extent analogous to those of some known Ub-binding domains, such as UBA, CUE, and UIM domains (12). All of these domains bind Ub on the surface centered by the Ile[44] residue of Ub. The UBA and CUE domains are structurally homologous, with a common three-helix bundle structure. UBA (from BMSC-UbP) binds Ub through its α1- and α3-helices as well as the loop between α1 and α2 (Fig. 7*B*) (30), whereas CUE (from Cue2-1) uses the α1- and α3-helices for the binding (Fig. 7*C*) (31). The single-helical UIM binds Ub through the conserved alanine neighbored by some hydrophobic residues, closely contacting with Ile[44] of Ub (Fig. 7*D*) (19). The binding surfaces of double-sided UIM (DUIM) (32) and the inverted UIM (MIU) (33, 34) are similar to that of normal UIM. The major difference of PFUC binding with Ub is that the flexibility of the P77 loop that considerably affects its Ub binding affinity. Besides, other Ub-binding domains have been identified with different binding patterns. The PHD fold of Pru domain from Rpn13 subunit of proteasome binds the common hydrophobic pocket of Ub through exclusive loops (35, 36). However, the GLUE domain from ESCRT-II EAP45 binds the Ile[44]-containing surface of Ub through the residues within secondary structural elements including C-terminal helix (37), although it also adopts a PHD fold.

The PFUC-binding surface on Ub is comprised of several hydrophobic residues centered by Ile[44]. There are high sequence similarity (58% identity) and structural similarity between NEDD8 and Ub (29). The residues on the binding surface of Ub, including Ile[44], Val[70], Arg[42], and Leu[8], are all conserved in NEDD8, but this hydrophobic patch does not exist in SUMO-1. So, it is not surprising that NEDD8 has the binding affinity with PFUC as in the case of Ub binding, whereas SUMO-1 has not. On the other hand, the major difference between NEDD8 and Ub is the residue in position 72 (Ala in NEDD8 and Arg in Ub), which is the main determinant of their selectivity in E1 recognition (38, 39) and deNEDDylating process (40). In this regard, the hydrophobic patch centered by Ile[44] may be the major source for the binding selectivity of Ub-like proteins or domains with the PFU domain of PLAA.

In summary, we have provided the solution structure and binding mode of a novel Ub-binding domain from human PLAA. Although the function of PLAA remains largely unknown, it is most likely that its major cellular function, similar to that of its counterpart DOA1 in yeast, is correlated with Ub binding. The Ub recognition by the PFU domain confers PLAA to function in cellular processes, such as mediating ERAD (4), controlling the concentration of free Ub in cells (41), regulating monoubiquitination for DNA repair (10), and sorting ubiquitinated membrane proteins into multivesicular bodies (11). Despite the weak binding of PFU with mono-Ub, it may bind poly-Ub cooperatively, and its Ub binding ability would be improved significantly. In this regard, the PFU domain may work as a recognition signal in all the above-mentioned processes. Whether binding of PFUC with poly-Ub or full-length PLAA with Ub provides a stronger affinity remains to be elucidated in the future.

Acknowledgments—We thank Dr. Yong-Gang Chang for critical reading of the manuscript and Drs. Yong Wang and Fang Zhang for technical assistance.

REFERENCES

1. Lord, J. M., Roberts, L. M., and Stirling, C. J. (2005) *Curr. Biol.* **15,** R963–964
2. Römisch, K. (2005) *Traffic* **6,** 706–709
3. Meusser, B., Hirsch, C., Jarosch, E., and Sommer, T. (2005) *Nat. Cell Biol.* **7,** 766–772
4. Raasi, S., and Wolf, D. H. (2007) *Semin. Cell Dev. Biol.* **18,** 780–791
5. Decottignies, A., Evain, A., and Ghislain, M. (2004) *Yeast* **21,** 127–139
6. Ghislain, M., Dohmen, R. J., Levy, F., and Varshavsky, A. (1996) *EMBO J.* **15,** 4884–4899
7. Mullally, J. E., Chernova, T., and Wilkinson, K. D. (2006) *Mol. Cell. Biol.* **26,** 822–830
8. Rumpf, S., and Jentsch, S. (2006) *Mol. Cell* **21,** 261–269
9. Russell, N. S., and Wilkinson, K. D. (2004) *Biochemistry* **43,** 4844–4854
10. Lis, E. T., and Romesberg, F. E. (2006) *Mol. Cell. Biol.* **26,** 4122–4133
11. Ren, J., Pashkova, N., Winistorfer, S., and Piper, R. C. (2008) *J. Biol. Chem.* **283,** 21599–21611
12. Hurley, J. H., Lee, S., and Prag, G. (2006) *Biochem. J.* **399,** 361–372
13. Bao, W. J., Gao, Y. G., Chang, Y. G., Zhang, T. Y., Lin, X. J., Yan, X. Z., and Hu, H. Y. (2006) *Protein Expr. Purif.* **47,** 599–606
14. Hu, H. Y., Horton, J. K., Gryk, M. R., Prasad, R., Naron, J. M., Sun, D. A., Hecht, S. M., Wilson, S. H., and Mullen, G. P. (2004) *J. Biol. Chem.* **279,** 39736–39744
15. Cornilescu, G., Delaglio, F., and Bax, A. (1999) *J. Biomol. NMR* **13,** 289–302
16. Rieping, W., Habeck, M., Bardiaux, B., Bernard, A., Malliavin, T. E., and Nilges, M. (2007) *Bioinformatics* **23,** 381–382
17. Laskowski, R. A., Rullmannn, J. A., MacArthur, M. W., Kaptein, R., and Thornton, J. M. (1996) *J. Biomol. NMR* **8,** 477–486
18. de Vries, S. J., van Dijk, A. D., Krzeminski, M., van Dijk, M., Thureau, A., Hsu, V., Wassenaar, T., and Bonvin, A. M. (2007) *Proteins* **69,** 726–733
19. Wang, Q., Young, P., and Walters, K. J. (2005) *J. Mol. Biol.* **348,** 727–739
20. Fujiwara, K., Tenno, T., Sugasawa, K., Jee, J. G., Ohki, I., Kojima, C., Tochio, H., Hiroaki, H., Hanaoka, F., and Shirakawa, M. (2004) *J. Biol. Chem.* **279,** 4760–4767
21. Berke, S. J., Chai, Y., Marrs, G. L., Wen, H., and Paulson, H. L. (2005) *J. Biol. Chem.* **280,** 32026–32034
22. Hofmann, K., and Falquet, L. (2001) *Trends Biochem. Sci.* **26,** 347–350
23. Fisher, R. D., Wang, B., Alam, S. L., Higginson, D. S., Robinson, H., Sundquist, W. I., and Hill, C. P. (2003) *J. Biol. Chem.* **278,** 28976–28984
24. Swanson, K. A., Kang, R. S., Stamenova, S. D., Hicke, L., and Radhakrishnan, I. (2003) *EMBO J.* **22,** 4597–4606
25. Ryu, K. S., Lee, K. J., Bae, S. H., Kim, B. K., Kim, K. A., and Choi, B. S. (2003) *J. Biol. Chem.* **278,** 36621–36627
26. Schubert, M., Labudde, D., Oschkinat, H., and Schmieder, P. (2002) *J. Biomol. NMR* **24,** 149–154
27. Holm, L., and Sander, C. (1996) *Science* **273,** 595–603
28. Osipiuk, J., Górnicki, P., Maj, L., Dementieva, I., Laskowski, R., and Joachimiak, A. (2001) *Acta Crystallogr. D. Biol. Crystallogr.* **57,** 1747–1751
29. Whitby, F. G., Xia, G., Pickart, C. M., and Hill, C. P. (1998) *J. Biol. Chem.* **273,** 34983–34991
30. Chang, Y. G., Song, A. X., Gao, Y. G., Shi, Y. H., Lin, X. J., Cao, X. T., Lin, D. H., and Hu, H. Y. (2006) *Protein Sci.* **15,** 1248–1259
31. Kang, R. S., Daniels, C. M., Francis, S. A., Shih, S. C., Salerno, W. J., Hicke, L., and Radhakrishnan, I. (2003) *Cell* **113,** 621–630
32. Hirano, S., Kawasaki, M., Ura, H., Kato, R., Raiborg, C., Stenmark, H., and Wakatsuki, S. (2006) *Nat. Struct. Mol. Biol.* **13,** 272–277
33. Lee, S., Tsai, Y. C., Mattera, R., Smith, W. J., Kostelansky, M. S., Weissman, A. M., Bonifacino, J. S., and Hurley, J. H. (2006) *Nat. Struct. Mol. Biol.* **13,** 264–271
34. Penengo, L., Mapelli, M., Murachelli, A. G., Confalonieri, S., Magri, L., Musacchio, A., Di Fiore, P. P., Polo, S., and Schneider, T. R. (2006) *Cell* **124,** 1183–1195
35. Schreiner, P., Chen, X., Husnjak, K., Randles, L., Zhang, N., Elsasser, S., Finley, D., Dikic, I., Walters, K. J., and Groll, M. (2008) *Nature* **453,** 548–552
36. Husnjak, K., Elsasser, S., Zhang, N., Chen, X., Randles, L., Shi, Y., Hofmann, K., Walters, K. J., Finley, D., and Dikic, I. (2008) *Nature* **453,** 481–488
37. Alam, S. L., Langelier, C., Whitby, F. G., Koirala, S., Robinson, H., Hill, C. P., and Sundquist, W. I. (2006) *Nat. Struct. Mol. Biol.* **13,** 1029–1030
38. Walden, H., Podgorski, M. S., Huang, D. T., Miller, D. W., Howard, R. J., Minor, D. L., Jr., Holton, J. M., and Schulman, B. A. (2003) *Mol. Cell* **12,** 1427–1437
39. Souphron, J., Waddell, M. B., Paydar, A., Tokgöz-Gromley, Z., Roussel, M. F., and Schulman, B. A. (2008) *Biochemistry* **47,** 8961–8969
40. Shen, L. N., Liu, H., Dong, C., Xirodimas, D., Naismith, J. H., and Hay, R. T. (2005) *EMBO J.* **24,** 1341–1351
41. Johnson, E. S., Ma, P. C., Ota, I. M., and Varshavsky, A. (1995) *J. Biol. Chem.* **270,** 17442–17456